PETROLOGIC, ISOTOPIC AND ELEMENTAL CHARACTERIZATION OF SHOCK-MELTED INTERMEDIATE OLIVINE GABBROIC SHERGOTTITE NORTHWEST AFRICA 11509.

A. J. Irving[1], S. M. Kuehner[1], P. K. Carpenter[2], D. E. Moser[3], I. Barker[3], M. Righter[4], T. J. Lapen[4], D. Weimer[5], H. Busemann[5], K. Ziegler[6] and B. Hoefnagels [1]Dept. of Earth & Space Sciences, University of Washington, Seattle, WA 98195 (irvingaj@uw.edu), [2]Dept. of Earth & Planetary Sciences, Washington University, St. Louis, MO, [3]Dept. of Earth Sciences, Western University, London, Ontario, Canada, [4]Dept. of Earth & Atmospheric Sciences, University of Houston, TX, [5]ETH Zürich, Switzerland, [6]Institute of Meteoritics, University of New Mexico, Albuquerque, NM.

Introduction: A fresh 500 gram stone found in Mali is a relatively coarse grained gabbroic shergottite containing shock-melted intercumulus zones. Among the 108 unpaired Martian meteorites now recognized [1], only NWA 6342 exhibits some similar shock features.

Figure 1. *Whole NWA 11509 stone showing the phaneritic texture and vesicles. Photo courtesy A. Habibi.*

Primary Petrology: The specimen consists of relatively equant grains of clinopyroxene and olivine (grainsize 1.4-3 mm) with vesicular, plagioclase-rich interstitial regions (see Figures 1, 2, 3). The mineral mode determined from a back-scattered electron mosaic is 50.5 vol.% clinopyroxene, 20.1 vol.% plagioclase, 17.1 vol.% olivine, 11.1 vol.% vesicles, 1.0 vol.% oxides (chromite + ilmenite) and 0.2 vol.% pyrrhotite. Clinopyroxene -- comprising both pigeonite ($Fs_{26.3-36.1}Wo_{6.4-21.7}$; FeO/MnO = 26-34) and subcalcic augite ($Fs_{19.8-27.2}Wo_{33.3-32.9}$, FeO/MnO = 25-32) -- and olivine ($Fa_{37.9-57.0}$, FeO/MnO = 50-55) exhibit rather limited compositional zoning. Olivine has been recrystallized into aggregates of ultra-fine grained polygonal subgrains (see Figure 4). Some plagioclase (which is *not* maskelynite) has a curved lath-like habit. Chromite has variable Ti content and some pyrrhotite contains minor Ni.

Shock-Produced Interstitial Zones: This specimen is remarkable for the presence of complex interstitial zones (perhaps originally intercumulus) containing two separate components (see Figure 5). The dominant component consists of fine grained birefringent, polycrystalline plagioclase ($An_{56.0-60.7}Or_{1.8-0.7}$) intergrown with subordinate prismatic low-Ca pyroxene. The other component occurs as spheroidal to irregular "blobs" with quench texture composed of blocky grains of zoned ferroan olivine ($Fa_{54.3-75.4}$, FeO/MnO = 53-57), acicular grains of more sodic plagioclase ($An_{45.0}Or_{2.1}$), zoned clinopyroxene ($Fs_{32.2-57.8}Wo_{28.6-22.1}$, FeO/MnO = 34), chromite, ilmenite, pyrrhotite and rare merrillite.

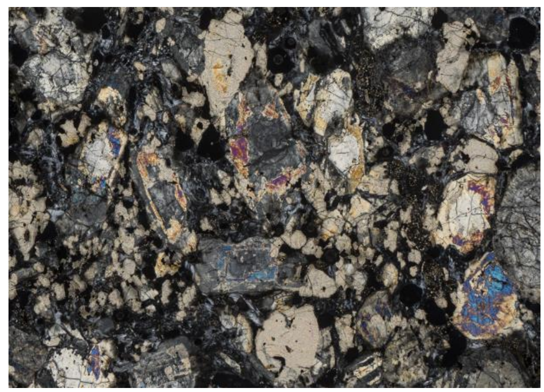

Figure 2. *Cross-polarized thin section image (width 1.2 cm). Rounded grains with anomalously low birefringence are polycrystalline olivine; rectangular grains are pyroxene; plagioclase+vesicles are dark.*

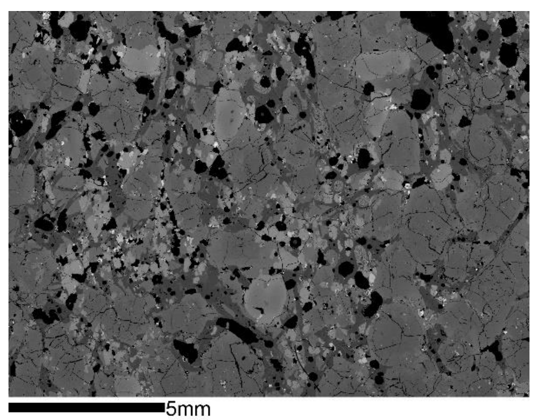

Figure 3. *Large area BSE image. Olivine (light gray), pyroxene (medium gray), plagioclase-rich interstitial regions (dark gray), vesicles (black), sulfide (bright).*

Oxygen Isotopes: Replicate analyses of acid-washed interior material by laser fluorination gave, respectively, $\delta^{17}O$ 2.623, 2.564. 2.685; $\delta^{18}O$ 4.514, 4.401, 4.640; $\Delta^{17}O$ +0.240, +0.240, +0.235 per mil.

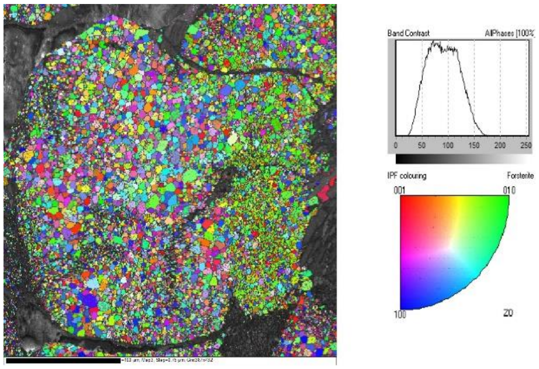

Figure 4. *EBSD image of a typical low birefringent olivine grain now composed of myriad polygonal subgrains with random crystallographic orientations. Red denotes c-axes perpendicular to page; likewise blue and green denote a-axes and b-axes, respectively.*

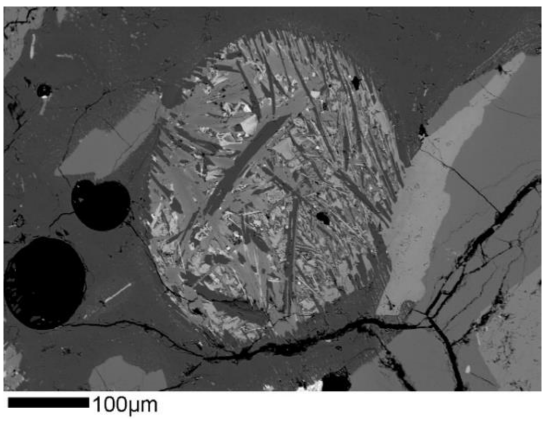

Figure 5. *BSE image of quench-textured magmatic "blob" within vesicular plagioclase (+ pyroxene) assemblage in shock-melted interstitial zone.*

Table 1. Whole Rock Elemental Abundances

SiO_2	(51.6)	La	1.11	Ba	31
TiO_2	0.44	Ce	2.82	Sr	31
Al_2O_3	5.37	Pr	0.43	Rb	1.6
Cr_2O_3	0.39	Nd	2.28	Sc	23.4
FeO	19.63	Sm	1.03	V	159
MnO	0.32	Eu	0.41	Ni	110
MgO	13.90	Gd	1.70	Zn	43
CaO	7.33	Tb	0.31	Y	8.9
Na_2O	0.54	Dy	2.09	Zr	27
K_2O	0.00	Ho	0.43	Hf	0.98
P_2O_5	0.46	Er	1.22	Th	0.21
SUM	100.0	Yb	1.08	U	0.13
mg	0.558	Lu	0.15	S	1390

Bulk Major and Trace Elements: Clean representative dust produced by cutting a sample on an Isomet saw using a Cu alloy blade was analyzed for major elements (in wt.%, by ICP-OES) and trace elements (in ppm, by QQQ-ICP-MS) at the University of Houston (Table 1). The REE pattern is parallel to and in the range of those for ITE-intermediate specimens.

Radiogenic Isotopic Compositions: Clean interior material was spiked for Lu-Hf and Sm-Nd analyses, microwave digested in $HF-HNO_3$ and measured by MC-ICP-MS. In spite of the whole rock REE signature, the $^{176}Hf/^{177}Hf$ ratio of 0.282940 ($\varepsilon Hf = +5.82$) plots *between* the established fields for intermediate and enriched shergottites [2]. Sm-Nd analyses are underway.

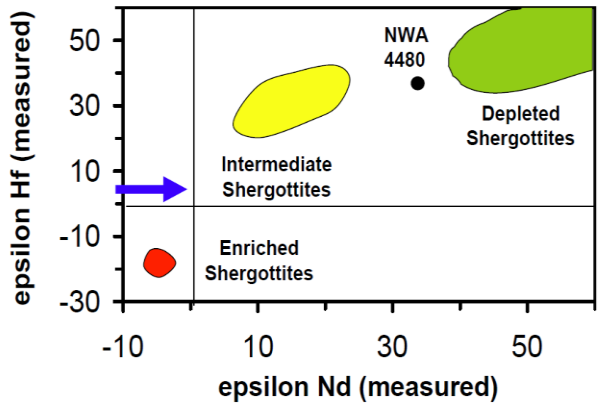

Figure 6. *Radiogenic isotopic compositions of shergottites (data from [3-5] and our unpubl. analyses). The Hf isotopic ratio for NWA 11509 (arrow) implies derivation from a unique Martian mantle source unlike those yielding other "intermediate" shergottites.*

Noble Gases and Cosmic Ray Exposure Age: A sample measured at ETH gave preliminary CRE ages (^3He 2.7 Myr, ^{21}Ne 3.0 Myr) similar to those for many other intermediate shergottites [6].

Concluding Remarks: NWA 11509 is a unique permafic non-poikilitic olivine gabbroic shergottite (possibly a magmatic cumulate) with intermediate ITE affinities but an aberrant Hf isotopic composition. Polycrystalline olivine, which was also recognized in intermediate shergottite NWA 6342 [7], implies high temperature thermal annealing of shock-deformed grains. Rapid crystallization of interstitial, shock-produced vesicular melts resulted in regions of intergrown plagioclase+low-Ca pyroxene, as well as possibly immiscible "blobs" of residual evolved liquid, which in turn quenched rapidly to aggregates of skeletal grains.

References: [1] http://www.imca.cc/mars/martian-meteorites-list.htm [2] Symes S. et al. (2008) *GCA* **72**, 1696-1710; Lapen T. et al. (2017) *Science Advances* **3**, doi: 10.1126/sciadv.1600922 [3] Irving A. et al. (2015) *LPS* **XLVI**, #2290 [4] Irving A. et al. (2016) *LPS* **XLVII**, #2330 [5] Irving A. et al. (2017) *LPS* **XLVIII**, #2068 [6] Wieler R. et al. (2016) *MaPS* **51**, 407-428 [7] Irving A. et al. (2011) *LPS* **XLII**, #1612.